

killed between the barriers. The sooner they finish what live coral remains, the sooner death through starvation will occur. It is important that this happen prior to the influx of larvae in the fall, or control activities may have to be extended for an additional year.

Destruction of living coral reefs would be an economic disaster for small isles and atolls of Oceania. Most inhabitants of Oceania derive almost all their protein from marine resources, and destruction of living reefs results in the destruction of fisheries. Eventually, loss of living corals would allow severe land erosion by storm waves.

Information concerning infestations in other areas of the Pacific is urgently needed. Reports of infestations have come from islands off Mersing on the east coast of Malaysia, from Borneo, New Guinea, Fiji Islands, Truk, Palau, Yap, Rota, Sipan, Wake, Johnston Island, the Great Barrier Reef, Midway, and Guam. With the exception of Guam, Australia, and Palau, the extent of the infestations is not known. Guam's infestation began only a little more than 2 years ago. Palau is in an early stage of infestation. Truk has had a heavy infestation for less than a year. Researchers working in the Pacific are requested to notify the author of normal populations or abnormal concentrations of *A. planci* and the degree of coral damage. Pertinent data on recent dredging or blasting activities or dynamiting for fish should be noted.

Long-term control may be possible by monitoring of areas subject to blasting or dredging during periods of larval settlement. Seed populations can be eliminated before larval settlement in the following year. If, however, the population explosion is due to a basic change in the life history of *A. planci*, control will probably not be possible. Geological records clearly indicate that large groups of animals have become extinct within a relatively short time. Rugose corals offer an excellent example. The appearance of an overly efficient predator might cause such extinction. Wholesale destruction of madreporarian corals has been witnessed during the past few years. This destruction may continue to the point where the coral fauna cannot recover. There is a possibility that we are witnessing the initial phases of extinction of madreporarian corals in the Pacific.

RICHARD H. CHESHER
University of Guam, Agana, Guam

18 JULY 1969

References and Notes

1. T. F. Goreau, *Bull. Sea Fish. Res. Sta. Haifa* **35**, 23 (1963).
2. J. H. Barnes, *Aust. Nat. Hist.* **15**, 256 (1966); D. E. Williamson, *Skin Diver* **17** (No. 3), 26 (1968); J. Harding, *Sea Frontiers* **14** (No. 5); 258 (1968).
3. R. H. Chesher, *Skin Diver* **18** (No. 3), 34, 84 (1969).
4. W. R. Coe, *J. Mar. Res.* **16**, 212 (1956).
5. R. Randall, University of Guam, unpublished field notes.
6. R. Endean, University of Queensland, personal communication.
7. M. B. Dell, *Trans. Amer. Fish. Ass.* **97** (No. 1), 57 (1968).
8. G. Thorson, *Trans. N.Y. Acad. Sci. Ser. 2* (No. 8), 693 (1956).
9. I thank Capt. Grieve and Capt. Wideman of the U.S. Navy for logistic support during the course of this project, and members of the University of Guam's Division of Marine Studies and Biosciences, and civilian and military scuba divers who provided considerable aid. Support was obtained through Resolution No. 519 (6-S) passed by a special session of the 9th Guam Legislature.

20 May 1969

Y-Modulation: An Improved Method of Revealing Surface Detail Using the Scanning Electron Microscope

A Stereoscan Mark II scanning electron microscope is now in use in the geology department of Imperial College of Science and Technology. Until now, the instrument has been used for looking at, and photographing, a variety of subjects from the realms of paleobotany, micropaleontology, biology, chemical technology, and metallurgy. This parallels work in progress on similar instruments elsewhere.

Recently, the instrument was fitted

with several accessories newly developed by the manufacturers (Cambridge Instrument Company). These include the so-called scan rotation unit, which has several functions. In addition to the ability to rotate the direction of scan through 360° and to compensate for the apparent distortion introduced by the angle of tilt of the specimen table, it incorporates a magnification factor, continuously variable from $\times 1$ to $\times 2.5$, and the Y-modulation device which is the subject of this report.

As in normal scanning electron microscopy, a finely focused beam of electrons is deflected across the surface under investigation. The number of electrons back-scattered and emitted is a function of the topography and composition of the specimen (see Fig. 1); such electrons are accelerated by a wire grid biased to +12 kv and allowed to strike the surface of a phosphor screen. The scintillation produced is viewed and amplified by a photomultiplier and the output of the photomultiplier is applied to a cathode-ray tube scanning in synchronization. The scan size of the cathode-ray tube remains fixed at 10.5 cm², but the area of scan on the specimen may be successively decreased, thus giving an apparent step-up of magnification within the range of $\times 20$ to $\times 100,000$ at the normal working distance of 11 mm. These values may be varied either by changing the working distance or by utilizing the zoom magnification factor on the scan rotation unit.

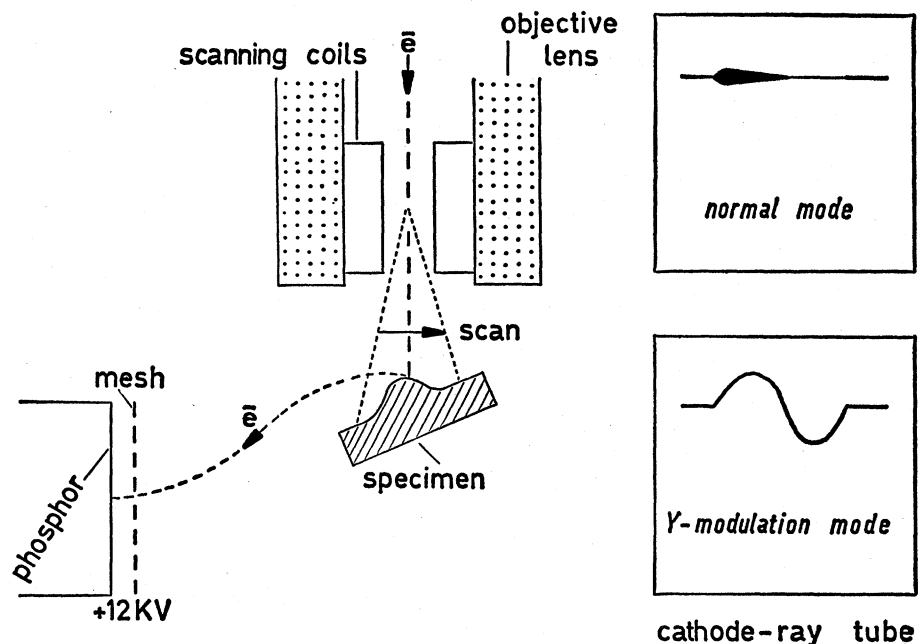


Fig. 1. Comparison between normal mode and Y-modulation mode as a function of topography.

In the normal mode the output modulates the intensity of the beam, but in the Y-modulation mode the output is used to deflect the line scan of the cathode-ray tube in the Y-direction, thus producing a pattern analogous to an X-Y recording. The image produced on the cathode-ray tube is photographed in each case.

If the line and frame speeds are synchronized to give 1000 lines per picture, an image corresponding to the topography of the surface is produced.

If the line and frame speeds are desynchronized, that is, high frame speed and low line speed, as few as 15 lines per frame can be displayed. If this is used in conjunction with a more detailed photograph, it allows the topographical variation of specific areas to be examined in considerable detail. One other feature should be mentioned at this point—the amplitude of modulation can be varied, thereby exaggerating or diminishing the topography. Thus a specimen which has indistinct

surface detail can produce an image of remarkable clarity when viewed by means of the Y-modulation device. Large amplitudes of modulation, however, produce an apparent Y-shift proportional to the relief; this can be minimized by using less modulation (see Figs. 2 and 3).

This method offered a solution to the problem encountered recently at Imperial College when the surface morphology of synthetic crystals of chalcopyrite on a magnetic substrate had to be examined with the Stereoscan.

It is normally impossible to obtain a good image from magnetic specimens, since the magnetic field of the specimen interferes with the focusing; a moderate focus can normally be achieved by using an astigmatic beam to compensate partially for this effect. Even so, in many cases, a clear image cannot be obtained at magnifications greater than about $\times 500$. Figures 4 and 5, which are taken at a magnification of $\times 2600$, demonstrate the increased clarity obtained by the use of Y-modulation.

Chalcopyrite crystallizes below 550°C in class $42m$ of the tetragonal system and has a crystalline structure very similar to the well-known cubic mineral sphalerite (ZnS). Numerous growth steps, unequal face developments, and frequent twinning complicate the morphologies of most of the synthetic crystals but the predominance of the general forms—the $\{112\}$ and $\{1\bar{1}2\}$ bisphenoids—is revealed in the frequency of faces with more or less regular triangular and hexagonal outlines; bipyramidal modifications are not uncommon but other forms seem to be rare or absent. In addition to multiple growth steps, many faces exhibit very small spots that occur both haphazardly and along lines parallel to growth steps on a single surface. Other crystal habits are also illustrated (Figs. 4 and 5), including large platy, and columnar, needlelike growths.

The improvement obtained by Y-modulation is best demonstrated by Figs. 6 and 7, which show some growth structures found on a sphenoidal surface of chalcopyrite. Low relief, more or less hexagonal, positive features in the larger flat area (Fig. 7) appear to be outgrowths from nucleation points that will eventually coalesce to form another crystal layer. The ease of nucleation on surface discontinuities is shown in the concentration and exaggerated growth of similar features along striae formed by the intersection of

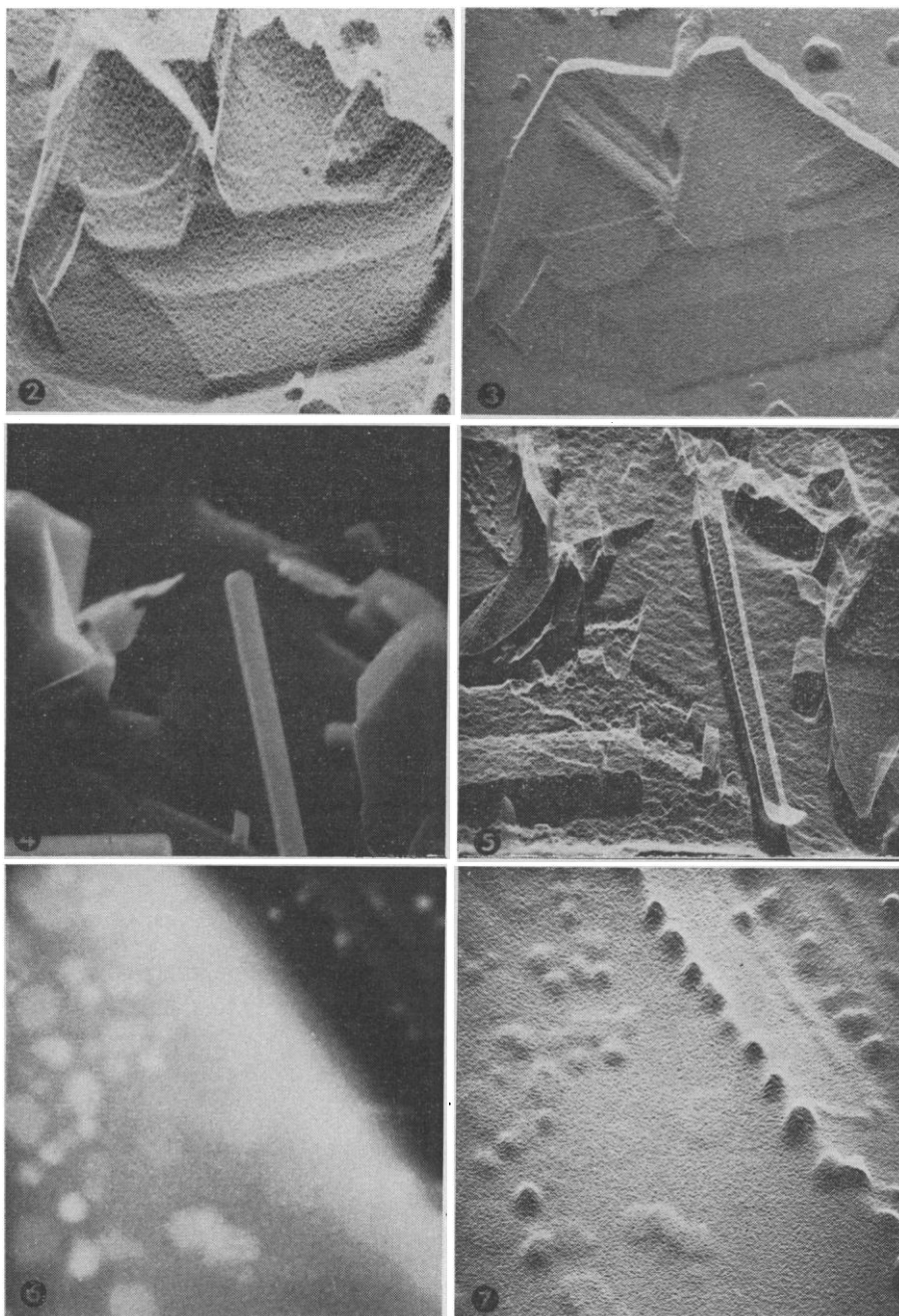


Fig. 2. Synchronized Y-modulation image (100 percent modulation) ($\times 2700$). Fig. 3. Synchronized Y-modulation image (20 percent modulation) ($\times 2700$). Fig. 4. Normal mode image of columnar crystal ($\times 1400$). Fig. 5. Y-modulation mode image of Fig. 4 (100 percent modulation). Fig. 6. Normal mode image of surface structures on a sphenoidal surface of chalcopyrite ($\times 15,000$). Fig. 7. Y-modulation mode image of Fig. 6 (100 percent modulation).

other sphenoidal planes with the surface. Most of this detail is invisible in Fig. 6, although the hexagonal outline of the surface structures is sometimes quite distinct.

The clarity with which the step-by-step growth features can be observed (see cover, upper right) is further exemplified at a magnification which, in the normal mode (cover, upper left), is clearly unusable. Taken at lower power (cover, lower left and lower right), the Y-shift effect can be seen to introduce considerable difficulties in interpretation if complex morphology or topographical relief is present. Using a lower amount of modulation will reduce this effect (as shown previously, Figs. 2 and 3), but, taken in conjunction with the normal mode photograph, the Y-modulation mode photograph permits detailed examination of fine structure of selected areas.

We thus deduce that this method becomes increasingly important as higher and higher magnifications are employed, especially with magnetic materials or on surfaces with low or moderate relief, and that at lower magnification the Y-modulation photographs provide valuable information supplementing normal mode photographs.

There are many possible applications

of the use of this device—for example, examining and photographing the morphology and surface structure of very small crystals, such as those encountered in clay mineralogy. Stereo pairs made by this means will also be exceptionally useful.

Further, the Stereoscan may now be fitted with a spectrometer, and therefore be capable of electron-probe microanalysis. Under these conditions the output of the x-ray detector may be applied to the line scan in lieu of the photomultiplier output; this will produce a Y-modulation image which represents the distribution of the elements in the specimen analyzed in a three-dimensional form.

Finally, the scanning electron microscope will soon be fitted with a self-heating stage. This will enable us to examine magnetic minerals while heating them through their Curie points and to observe any changes taking place at that temperature.

T. K. KELLY
W. F. LINDQVIST

*Department of Mining Geology,
Royal School of Mines, Imperial
College, London, S.W.7, England*

M. D. MUIR

Department of Geology

6 February 1969

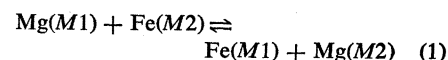
Cooling History of Orthopyroxenes

Abstract. *Order-disorder transitions between ferrous iron and magnesium in orthopyroxenes [minerals close to the composition $(Fe,Mg)SiO_3$] occur rapidly between approximately 480° and 1000°C. Disordering and ordering have been studied experimentally. The determination of the metastable ferrous iron site occupancy in orthopyroxenes from rapidly cooled volcanic rocks provides information on the cooling rates, especially from 600° to 480°C.*

Atomic order-disorder transitions in silicate crystals are often very sluggish. If the temperature changes rapidly, the atomic distribution over the nonequivalent sites may not be in accord with the equilibrium state at any instant. Below a critical temperature, the time needed to reach equilibrium will be very long and geological times may be needed to accomplish an equilibrated distribution. This is of special interest for the earth scientist since nonequibrated site occupancies may be found in nature which permit conclusions on the cooling history of the mineral. We have found that Fe^{2+},Mg order-disorder in orthopyroxenes is an unusually simple example which can be approached from the point of view of simple thermodynamical considerations.

Some features, however, are quite different from the order-disorder phenomena in silicates.

Orthopyroxenes are orthorhombic minerals with chemical compositions which represent a quasi-binary solution close to the join between $FeSiO_3$ and $MgSiO_3$. The ferrous and magnesium ions occur at two nonequivalent, octahedrally coordinated sites $M1$ and $M2$, with Fe^{2+} preferring $M2$. The cation exchange is formulated by the simple relation



The energy difference between the two opposing reactions determines the temperature range in which ordering and disordering will occur under equilib-

rium conditions. If the activation energy needed to overcome the barriers for cationic diffusion within the crystal structure is high, the time necessary to reach equilibrium will be long. No change of lattice symmetry occurs in this simple order-disorder transition.

We have determined precise site occupancy numbers for Fe^{2+} at $M1$ and $M2$ from the quadrupole split doublets of ^{57}Fe observed in gamma-ray resonant absorption spectra at 77°K (1). Orthopyroxenes with various compositions were heat-treated at different temperatures. The data were analyzed as follows. The fraction of Fe^{2+} at $M1$ and $M2$ is proportionally related to the ratio of the areas under the two doublets provided that thin absorbers are used and the recoilless fraction of ^{57}Fe is the same at both sites. Four Lorentzian curves were fitted to the data by the least-squares method (13 variable fits). A careful analysis of many spectra showed that the intrinsic widths of all four peaks are very nearly the same. Therefore, since peak heights are determined much more precisely than line widths, ratios of the peak heights were used rather than ratios of the product of peak height times width. Data for one orthopyroxene are given in Table 1 (which shows three spectra of the same absorber).

Figure 1 shows the equilibrium Fe^{2+},Mg distribution over sites $M1$ and $M2$ at 1000°C. In the range $0 \leq x < 0.6$, where x is the ratio $Fe^{2+}/(Fe^{2+} + Mg)$ of the crystal, the observed site occupancy is in excellent agreement with ideal distribution assumed for each site (2, 3). The site occupancy numbers X_1 and X_2 for Fe^{2+} at $M1$ and $M2$, respectively, are in accordance with the hyperbolic relation

$$k = X_1(1 - X_2)/X_2(1 - X_1) \quad (2)$$

where k is the equilibrium constant. In the region $0.7 < x \leq 1.0$ (Fig. 1), there is a typical deviation from ideal distribution. At 1000°C, orthopyroxenes are still far from completely disordered. No additional disorder could be observed, however, when crystals were heated at higher temperatures. Equilibrium values of order-disorder were also determined for a sample with $x = 0.574$ at 800°, 700°, 600°, and 500°C. The variation of the site occupancy number X_2 with temperature is shown in Fig. 2.

Data for orthopyroxenes from slowly annealed metamorphic and plutonic rocks are plotted in Fig. 1. These samples exhibit site occupancy numbers close to an equilibrium distribution